Noncontact Cohesive Swimming of Bacteria in Two-Dimensional Liquid Films

Ye Li,[1] He Zhai,[2] Sandra Sanchez,[3] Daniel B. Kearns,[3] and Yilin Wu[1,*]

[1]*Department of Physics and Shenzhen Research Institute, The Chinese University of Hong Kong,
Shatin, New Territories, Hong Kong, People's Republic of China*
[2]*Northwest Institute For Nonferrous Metal Research, 96 Weiyang Street, Xian, Shaanxi 710016, People's Republic of China*
[3]*Department of Biology, Indiana University, 1001 East 3rd Street, Bloomington, Indiana 47405, USA*

Bacterial swimming in confined two-dimensional environments is ubiquitous in nature and in clinical settings. Characterizing individual interactions between swimming bacteria in 2D confinement will help to understand diverse microbial processes, such as bacterial swarming and biofilm formation. Here we report a novel motion pattern displayed by flagellated bacteria in 2D confinement: When two nearby cells align their moving directions, they tend to engage in cohesive swimming without direct cell body contact, as a result of hydrodynamic interaction but not flagellar intertwining. We further found that cells in cohesive swimming move with higher directional persistence, which can increase the effective diffusivity of cells by ∼3 times as predicted by computational modeling. As a conserved behavior for peritrichously flagellated bacteria, cohesive swimming in 2D confinement may be key to collective motion and self-organization in bacterial swarms; it may also promote bacterial dispersal in unsaturated soils and in interstitial space during infections.

The motile behavior of bacteria is of great ecological and medical significance because it is essential for bacterial dispersal, chemotaxis, and pathogenesis. A large number of bacterial species use flagellar motility to propel their motion [1]. Flagellar motility has been studied extensively in various environments, both in bulk fluids [1–6] and under quasi-2D confinement [7–15]. By contrast, flagellar motility in "strictly" 2D confinement with a thickness close to cell width (∼2 microns or smaller) is less well understood. Individual swimming behavior of bacteria in 2D confinement has received significant recent attention from theorists [14,16,17], but has only been qualitatively described in experiments [18–20].

Characterizing bacterial swimming behavior and interactions in 2D confinement will help to understand diverse microbial processes in the natural environment and in clinical settings, such as bacterial swarming [21–26], biofilm formation [27,28], bacterial dispersal in unsaturated soils [29,30], and pathogen spreading in the interstitial fluid of animal tissues [31–34]. Moreover, the accurate characterization of individual bacterial interactions in 2D confinement is essential to the understanding of how single cell behavior leads to collective dynamics in bacterial swarms, a question of direct relevance to active matter self-organization [21,35–38] and low-Reynolds number hydrodynamics [2,39]. Steric repulsion and flagellar intertwining were believed to dominate individual interactions between swimming bacteria in proximity [19,40], and steric repulsion was suggested to be a key mechanism responsible for self-organization in quasi-2D bacterial suspensions [9,11,12, 20,41]. However, it is unclear whether these conclusions are applicable to bacteria swimming in 2D confinement.

Here we report a novel motion pattern displayed by flagellated bacteria in 2D confinement, i.e., cohesive swimming between nearby cells that involves neither steric repulsion nor flagellar intertwining. To observe this phenomenon, we developed a simple yet highly robust and reproducible method to confine low-density bacterial populations in liquid films ∼2 microns in thickness (see Supplemental Material, methods [42]). We first allowed *B. subtilis* (DS1919 with wildtype flagellar motility, hereafter referred to as "wildtype" or "WT") to swarm on an agar surface to an appropriate colony size, and then cells at the swarm edge were diluted and transferred to fresh agar surface. The cells were then covered with a clean glass cover slip and observed by microscopy with careful control of humidity. We found that this method robustly produced a 2D dilute cell suspension confined between two no-slip walls, i.e., the agar surface and the glass cover slip, and the 2D suspension formed this way was maintained for ∼10 min before the fluid is absorbed by agar. Cells (0.8 μm in diameter, 7.3 ± 1.8 μm in length) moved vigorously at a speed of 52 ± 7 μm/s (mean ± s.d.) with suppressed tumbling [18] (see Supplemental Material, Fig. S1 [42]). They moved in curved trajectories with a bimodal curvature distribution [Supplemental Fig. S2(a) [42]], suggesting that they experienced equal hydrodynamic interactions with the two solid walls [14,51–53]. Importantly, cells remained in the same focal plane under the microscope, supporting the conclusion that their motion was restricted to two dimensions. We managed to control bacterial density at about 9.5×10^{-4} cells/μm^2, corresponding to an average cell-cell distance of ∼5 cell lengths and allowing occasional collision between cells.

Remarkably, when two cells aligned their moving directions as they approached or collided with each other, they tended to swim side by side cohesively without cell body
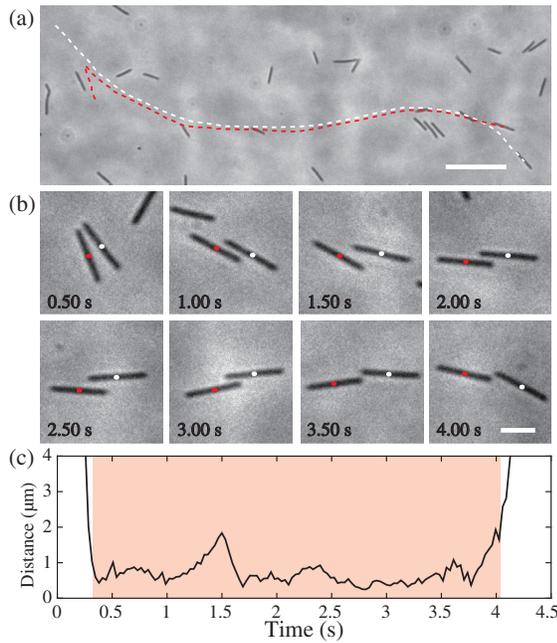
FIG. 1.   Noncontact cohesive swimming of bacteria. (a) Two wildtype *B. subtilis* cells approached each other and swam cohesively for ~3.7 s without direct cell body contact. Dashed lines represent trajectories of the two cells. Scale bar, 20 μm. Also see Supplemental Material, movie 1 [42]. (b) An image sequence of the zoomed-in view of the cell pair undergoing cohesive swimming in panel (a). The centers of the cell pair are labeled by white and red dots. Scale bar, 5 μm. (c) Nearest distance between the two cells in panel (a) plotted against time. The shaded area indicates the duration of cohesive swimming. The nearest distance is zero if two cells are in direct body contact.

contact for an extended distance up to ~200 μm [Fig. 1(a); Supplemental Material, movie 1 [42]]. The duration of noncontact cohesive swimming (i.e., the trapping time) was 1.10 ± 0.55 s [mean $\pm$ SD, $n = 94$; Fig. 2(a)]. During such cohesive swimming, the two cells typically remained separated by a nearest distance of 0.7 ± 0.4 μm, with the mean distance comparable to cell width (0.8 μm) [Fig. 1(b)]. The nearest distance between two cells at any instant was defined as the minimal distance between any two points belonging to different cells. It was computed with high precision via a series of steps of digital image processing: Briefly, we first determined the center position and orientation of cells via ellipse fit of cell boundary in thresholded images, then used this information to measure cell length or width and to reconstruct 3D cell profiles, and, finally, computed cell-cell distance based on the reconstructed cell profiles (Supplemental Material, methods and Fig. S3 [42]). The noncontact cohesive swimming we describe here is in stark contrast to the pairwise swimming behavior found in earlier reports that involved direct cell body contact throughout the swimming process [19]. Multicellular clusters consisting of three or more cells also displayed noncontact cohesive swimming (Supplemental Material, movie 2 [42]).
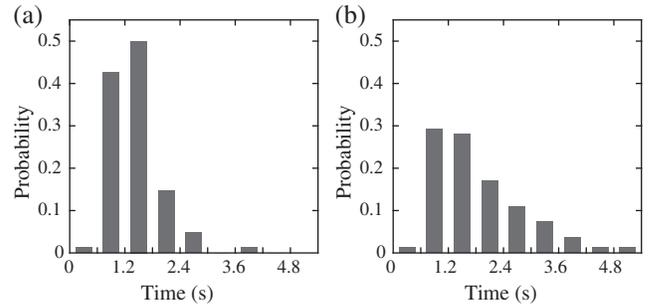
FIG. 2.   Probability distribution of trapping time for cohesively swimming cell pairs of *B. subtilis*. (a) Wildtype, (b) smooth-swimming mutant, bin size is 0.6 s. The trapping time is defined as the time duration traveled by two cohesively swimming cells before they separate spontaneously. Two cells are considered as engaging in cohesive swimming if the distance between their centers is less than their average length and if the angle between their velocity directions is less than 10°. The mean trapping time of wildtype and smooth-swimming *B. subtilis* is 1.10 ± 0.55 s (mean $\pm$ s.d., $n = 94$) and 1.55 ± 0.95 s (mean $\pm$ SD, $n = 82$), respectively.

Similar noncontact cohesive swimming behavior was found in *Escherichia coli* (Supplemental Material, movie 3 [42]) and in *Proteus mirabilis* (Supplemental Material, movie 4 [42]), both are Gram-negative bacteria with peritrichous flagella, suggesting that the behavior is conserved among peritrichously flagellated bacteria. Interestingly, *P. mirabilis* cells have a broad distribution of cell length, and those longer cells often recruit a number of shorter ones to perform noncontact cohesive swimming (Supplemental Material, movie 4 [42]).

Next we sought to understand the mechanism of the observed noncontact cohesive swimming behavior. Apparently, steric repulsion between cell bodies is not involved here. Note that flagellar filaments are thin (~20 nm in diameter, i.e., ~1/40 of cell width) and flexible, and they do not exert any steric force during cell-cell contact; for example, when *E. coli* cells swim in 2D liquid films, flagellar filaments and cell bodies belonging to different cells often overlap [54]. Nonetheless, flagellar intertwining can lead to two cells swimming cohesively through bulk fluids, and electron microscopy studies suggested that it may account for the formation of multicellular rafts or clusters during bacterial swarming [55,56]. To examine whether flagellar filaments of adjacent cells intertwined during the noncontact cohesive swimming, we used high speed fluorescence microscopy to visualize the motion of flagellar filaments of cohesively swimming cells in 2D confinement with wildtype *B. subtilis* (DS1919) and with a smooth-swimming mutant (mutated for *cheB* gene; DK2178) [42,54,57,58]. The *cheB* mutant moves at a similar speed as wildtype and displays noncontact cohesive swimming in 2D confinement, with a longer duration of cohesive swimming (1.55 ± 0.95 s, mean $\pm$ SD, $n = 82$; see Fig. 2(b) and Supplemental Material, Fig. S4 [42]). We found that wildtype cells display light-induced tumbling at
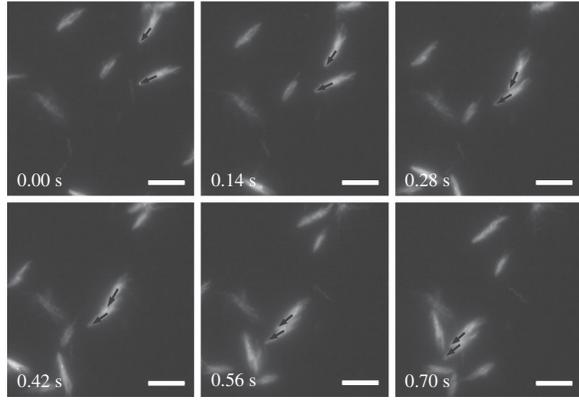
FIG. 3. Flagellar dynamics of two cells undergoing noncontact cohesive swimming. Flagellar filaments of *B. subtilis* DK2178 cells were fluorescently labeled and appeared bright in the image sequence. The two black arrows indicate the orientations of two cells that approached each other and traveled as a cohesive pair. Scale bar, 10 μm. See Supplemental Material, movie 6 [42].

wavelengths 400–600 nm, while the *cheB* mutant swims smoothly even under intense illumination at 400–650 nm, so the *cheB* mutant allows us to acquire much clearer images of flagellar rotation during cohesive swimming using green-light excited dyes with higher quantum yield. In both the wildtype and smooth-swimming mutant, we found that flagellar intertwining (i.e., formation of a flagellar cobundle) did not occur between two cells undergoing noncontact cohesive swimming, and their flagella bundles appeared to rotate independently (Fig. 3 and Supplemental Material, movies 5 and 6 [42]). The result showed that flagellar intertwining is not a mechanism for the noncontact cohesive swimming in 2D confinement. This is consistent with the report that swarm cells rarely engage in direct flagellar interaction [54].

Hydrodynamic interactions dominate over rotational diffusion for two swimming bacteria within a distance of one cell length [40]. We then sought to examine the contribution of hydrodynamic interactions to the noncontact cohesive swimming. A pusher-type flagellated swimmer such as *B. subtilis* and *E. coli* can be modeled as a force dipole which pushes fluid away from the body along the long axis and draws fluid toward the sides [2]. In 2D confinement this (screened) dipolar flow field results in short-range hydrodynamic attraction between two approaching cells, and the hydrodynamic attraction is counteracted by the orientational change of cell bodies due to effective rotational diffusion. This process is analogous to bacteria swimming near solid walls, in which case cells arrive at the wall with some angle, reorient to swim parallel to it for a while and eventually leave due to rotational diffusion. The process of cell interaction during cohesive swimming can be modeled as a swimmer interacting with its "mirror image" [40,52]. Two cohesively swimming cells in 2D confinement would undergo cohesive swimming for a finite duration (i.e., the trapping time) until separation when the angle between them reaches a critical

value $2\theta_c$, at which the effects of hydrodynamic attraction and of effective rotational diffusion are just balanced by each other. Here we used a similar approach as Drescher *et al.* and Spagnolie *et al.* took [40,52] to derive the trapping time for nontumbling cells.

Denoting the angle between two cohesively swimming cells as θ, the angular velocity arising from flow field generated by a nearby mirror cell is as follows (Supplemental Material [42]):

$$\dot{\theta} = -\frac{3F_pL}{64\pi\eta H^3}\sin\theta\cos\theta(1+\gamma\sin^2\theta). \qquad (1)$$

In Eq. [1] F_p is the propulsive force generated by rotating flagella, L is approximately the cell length ($\sim$7.3 μm), η is water viscosity, $2H$ is the distance between the centers of the two cells, and γ is related to the cell body aspect ratio. We obtained $F_p = 0.26 \pm 0.05$ pN by fitting cell alignment process during cell-cell collisions (Supplemental Material, Fig. S5 [42]), which agrees with the values measured by optical trap ($\sim$0.57 pN) [59] and predicted by resistive force theory (0.41 ± 0.23 pN) [60]. Equation (1) can be rewritten as

$$\dot{\theta} = -\frac{d}{d\theta}U(\theta), \qquad (2)$$

where $U(\theta)$ is the effective potential and it satisfies $U(0) = 0$. For *B. subtilis*, $\gamma \sim 1$, so we have

$$U(\theta) = \frac{3F_pL}{256\pi\eta H^3}(\cos^4\theta - 4\cos^2\theta + 3). \qquad (3)$$

Because $\theta < \theta_c$ and θ_c is very small, $U(\theta)$ can be approximately written as the following form:

$$U(\theta) \approx \frac{3F_pL\theta^2}{128\pi\eta H^3}. \qquad (4)$$

Taking rotational diffusion of cell orientation into account, Eq. (2) is rewritten as [40]

$$\dot{\theta} = -\frac{d}{d\theta}U(\theta) + (2D_r^{\mathrm{eff}})^{\frac{1}{2}}n(t), \qquad (5)$$

where D_r^{eff} is the effective rotational diffusion constant of cell orientation and $n(t)$ describes Gaussian white noise. Equation (5) describes the angular Brownian motion under the effect of potential $U(\theta)$. The time for a cohesive cell pair to separate from each other becomes a Kramers problem for the escape over a potential barrier $\Delta U = U(\theta_c)$ [40]. Solving the equation yields the trapping time

$$t \approx \left(\frac{\theta_c^2}{D_r^{\text{eff}}}\right) \exp\left(\frac{U(\theta_c)}{D_r^{\text{eff}}}\right). \qquad (6)$$

In Eq. (6), $D_r^{\text{eff}} = 0.23 \pm 0.02$ rad^2/s was obtained by fitting the mean square deviation of cell orientation over time to $\langle \Delta\theta^2 \rangle = 2D_r^{\text{eff}}t$; $\theta_c \approx 10°$ was obtained based on the criterion of cell separation (Supplementa Material [42]). With Eq. (4) and Eq. (6) we estimated the trapping time as 6 ± 2 s. Our estimate is consistent with the upper limit of the experimental result of the duration traveled by cohesively swimming cells (~4–5 s; Fig. 2). In experiment, the speed of cells often has a small variation, which causes cells to separate from each other more quickly than the ideal situation we modeled here. We conclude that the hydrodynamic interaction mediates noncontact cohesive swimming.

Next we sought to investigate the motion pattern of *B. subtilis* cells undergoing cohesive swimming. These cells swam at a mean speed (51 ± 8 μm/s, mean $\pm$ s.d.) similar to that of cells moving individually, but they displayed higher directional persistence as measured by the following autocorrelation function [Fig. 4(a)]:

$$C(\Delta t) = \langle \cos[\theta_i(t + \Delta t) - \theta_i(t)] \rangle. \qquad (7)$$

Here $[\theta_i(t + \Delta t) - \theta_i(t)]$ is the angle between velocity directions of the ith cell at time t and at time $t + \Delta t$; the angular brackets denote averaging over all tracked cells and over the time t. The higher directional persistence is also reflected in the narrower distribution of trajectory curvature for cells in cohesive swimming [Supplemental Material, Fig. S2(b) [42]]. Directional persistence of cells is governed by direction bias and rotational diffusion. Direction bias arises from the hydrodynamic interaction between cells and solid walls [14,51–53], which causes cells to swim in circles near boundaries, while rotational diffusion results from the combination of thermal Brownian rotation and the randomness of flagellar propulsion direction. Direction bias (denoted as B) and rotational diffusion constant (denoted as D_r) can be deduced from the mean square angular deviation $\Delta\theta$ that satisfies $\langle (\Delta\theta - Bt)^2 \rangle = 2D_r t$ (Supplemental Material [42]). Our measurement yielded $B = 0.38$ rad/s and $D_r = 0.035$ rad^2/s for cells in cohesive swimming, and $B = 0.72$ rad/s and $D_r = 0.043$ rad^2/s for cells moving individually. The direction bias of cells in cohesive swimming is only about half as much as that of cells moving individually, while the rotational diffusion constant is similar. So the higher directional persistence of cells in cohesive swimming is primarily due to reduced direction bias. To understand this result, we noticed that the flagellar bundles of two cells undergoing cohesive swimming in 2D confinement are expected to interact with the two solid walls independently and with equal probability. This is because flagellar bundles of the two cells rotate independently as suggested by flagellar visualization (Fig. 3), and because cells swimming individually interact with the
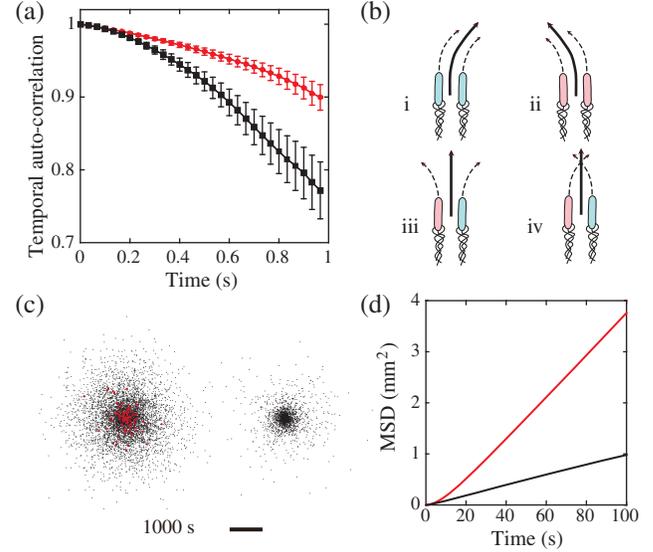
FIG. 4. (a) Auto correlation of cells' velocity direction measured in experiments. Red circles correspond to cells moving as cohesive pairs ($n = 126$ cells), and black circles correspond to individually moving cells ($n = 96$ cells). Bars represent standard error of the mean. (b) Illustration of 4 possible scenarios of cell-wall interaction for a pair of cells undergoing cohesive swimming. Cells colored in pink (or blue) interact with the upper (or lower) wall and tend to curve to the left (or to the right). The two cells in scenarios (iii) and (iv) interact with opposite walls, so the pair has reduced directional bias. (c) Spatial distribution of modeled cells with (left) and without (right) the ability to engage in cohesive swimming at the end of a typical simulation run. Red dots represent cells undergoing cohesive swimming and black dots represent cells moving individually. Note that a given cell alternates between the red and black state, with the frequency of the red state depending on collision rate (or local cell density), so at any specific time most cells in the red state are located in the inner region where cell density is higher. The duration of the simulation corresponds to cell dispersal for 1000 s. Scale bar, 5 mm. See Supplemental Material, movie 7 [42]. (d) Mean square displacement (MSD) of cells in simulations shown in (c). Red and black lines plot the average MSD ($n = 5$ independent simulation runs) for populations with and without the ability to engage in cohesive swimming, respectively.

two solid walls with equal probability as suggested by the nearly symmetric curvature distribution of cell trajectories [Supplemental Material, Fig. S2(a) [42]]. So there is a 50% chance for the two cells in cohesive swimming to interact with opposite walls at any instant, in which case the cell pair will have reduced directional bias [Fig. 4(b)]. Consequently, the mean direction bias of cells in cohesive swimming is reduced, resulting in the higher directional persistence [Fig. 4(b)].

Based on the above results, we reasoned that bacteria may enhance population dispersal in 2D confinement by engaging in cohesive swimming. To verify this idea, we built a stochastic computational model to simulate the dispersal dynamics of wildtype cells in 2D space (Supplemental Material [42]). When two modeled cells came close enough, they interacted

with each other either in the form of cohesive swimming or simple alignment, depending on their initial moving directions. Modeled cells were initially deposited at random positions within a circular area of radius 100 μm at the cell density found in our experiments (9.5×10^{-4} cells/μm^2); this circular area was referred to as the "virtual inoculums." To mimic the dispersal of bacteria from a source with unlimited supply of new cells, which may be relevant to the dispersal of bacteria from biofilms or from established infection sites, we kept cell density at the virtual inoculum as constant throughout simulations. Using experimentally obtained model parameters for wildtype *B. subtilis*, we simulated population dispersal and obtained the mean square displacement (MSD) of *all* cells outside the virtual inoculum as a function of time [Figs. 4(c), 4(d) and Supplemental Material, movie 7 [42]]. For comparison, the dispersal dynamics of cells without the ability to perform cohesive swimming was also simulated. By fitting the MSD plots in Fig. 4(d) with the numerical solution of 2D diffusion equation with the same boundary conditions as used in the simulations [61], we found that the effective diffusion coefficient (D) for wildtype cells ($D = 10.3 \times 10^3$ μm^2/s) is ~4 times greater than that of cells without the ability to engage in cohesive swimming ($D = 2.4 \times 10^3$ μm^2/s). These results show that the higher directional persistence of cells conferred by cohesive swimming can indeed facilitate population dispersal.

To summarize, we discovered that peritrichously flagellated bacteria in 2D confinement could engage in cohesive swimming in the absence of direct cell-to-cell contact. The noncontact cohesive swimming is mediated by hydrodynamic interaction but does not involve flagellar intertwining between cells. This motion pattern is not found in bulk fluids nor in quasi-2D liquid films, so it is unique to flagellated bacteria in 2D confinement. It provides new insight for understanding how single cell behavior lead to collective dynamics in 2D bacterial colonies, such as in bacterial swarms. Resembling the early stage of biofilm formation [22,27], bacterial swarms display rich dynamics of collective motion and self-organization [23,62]. These collective cellular behaviors contribute to multidrug tolerance of bacterial swarms [63–65], facilitate long-range material transport [24,66], and may promote invasiveness and virulence of infectious pathogens [67]. Here our results reveal that cohesive swimming mediated by short-range hydrodynamic attraction may be another key factor that gives rise to collective motion and self-organization in bacterial swarms, in addition to steric repulsion via direct contact of rod-shaped cells [20,68–70]. Moreover, our results suggest having larger cell aspect ratio would promote cohesive swimming, which may partially explain why some bacteria produce elongated cells during swarming [22].

The higher directional persistence conferred by noncontact cohesive swimming may promote bacterial dispersal in unsaturated soils and in interstitial space during infections, as these processes often occur in confined 2D

environments [29,32]. For example, *P. mirabilis* cells migrating in multicellular rafts (similar to those seen in our experiments; see Supplemental Material, movie 4 [42]) during catheter-associated urinary tract infections [55,67] may spread faster over the catheter surface with higher directional persistence as compared to cells moving individually. A similar example is well known in spermatozoa. Sperm of polyandrous species form cohesive groups due to hydrodynamics interaction between sperm cells [71,72]; these cohesive groups swim with higher linearity than individuals, allowing them to travel faster through the female reproductive tract [73]. Taken together, our results reveal noncontact cohesive swimming as a unique form of individual interaction between flagellated bacteria that may promote bacterial collective motion, self-organization, and dispersal in 2D environments.

*To whom correspondence should be addressed.
ylwu@phy.cuhk.edu.hk

[1] H. C. Berg, Phys. Today **53**, No. 1, 24 (2000).
[2] E. Lauga and T. R. Powers, Rep. Prog. Phys. **72**, 096601 (2009).
[3] L. Xie, T. Altindal, S. Chattopadhyay, and X.-L. Wu, Proc. Natl. Acad. Sci. U.S.A. **108**, 2246 (2011).
[4] Marcos H. C. Fu T. R. Powers, and R. Stocker, Proc. Natl. Acad. Sci. U.S.A. **109**, 4780 (2012).
[5] R. Rusconi, J. S. Guasto, and R. Stocker, Nat. Phys. **10**, 212 (2014).
[6] V. A. Martinez, J. Schwarz-Linek, M. Reufer, L. G. Wilson, A. N. Morozov, and W. C. K. Poon, Proc. Natl. Acad. Sci. U.S.A. **111**, 17771 (2014).
[7] X.-L. Wu and A. Libchaber, Phys. Rev. Lett. **84**, 3017 (2000).
[8] A. Sokolov, I. S. Aranson, J. O. Kessler, and R. E. Goldstein, Phys. Rev. Lett. **98**, 158102 (2007).
[9] L. H. Cisneros, J. O. Kessler, S. Ganguly, and R. E. Goldstein, Phys. Rev. E **83**, 061907 (2011).
[10] H. H. Wensink, J. Dunkel, S. Heidenreich, K. Drescher, R. E. Goldstein, H. Löwen, and J. M. Yeomans, Proc. Natl. Acad. Sci. U.S.A. **109**, 14308 (2012).
[11] A. Sokolov and I. S. Aranson, Phys. Rev. Lett. **109**, 248109 (2012).
[12] D. R. Shawn, S. Andrey, B. Leonid, and S. A. Igor, New J. Phys. **15**, 105021 (2013).
[13] T. Brotto, J.-B. Caussin, E. Lauga, and D. Bartolo, Phys. Rev. Lett. **110**, 038101 (2013).
[14] H. Shum and E. A. Gaffney, Phys. Rev. E **91**, 033012 (2015).

[15] J. Elgeti and G. Gompper, Europhys. Lett. **109**, 58003 (2015).

[16] M. Theers, E. Westphal, G. Gompper, and R. G. Winkler, Soft Matter **12**, 7372 (2016).

[17] T. Eisenstecken, J. Hu, and R. G. Winkler, Soft Matter **12**, 8316 (2016).

[18] S. A. Biondi, J. A. Quinn, and H. Goldfine, AIChE J. **44**, 1923 (1998).

[19] I. S. Aranson, A. Sokolov, J. O. Kessler, and R. E. Goldstein, Phys. Rev. E **75**, 040901 (2007).

[20] J.-M. Swiecicki, O. Sliusarenko, and D. B. Weibel, Integr. Biol. **5**, 1490 (2013).

[21] M. F. Copeland and D. B. Weibel, Soft Matter **5**, 1174 (2009).

[22] D. B. Kearns, Nat. Rev. Microbiol. **8**, 634 (2010).

[23] H. P. Zhang, A. Be'er, E.-L. Florin, and H. L. Swinney, Proc. Natl. Acad. Sci. U.S.A. **107**, 13626 (2010).

[24] Y. Wu, B. G. Hosu, and H. C. Berg, Proc. Natl. Acad. Sci. U.S.A. **108**, 4147 (2011).

[25] Y. Wu and H. C. Berg, Proc. Natl. Acad. Sci. U.S.A. **109**, 4128 (2012).

[26] G. Ariel, A. Rabani, S. Benisty, J. D. Partridge, R. M. Harshey, and A. Be'er, Nat. Commun. **6**, 8396 (2015).

[27] N. Verstraeten, K. Braeken, B. Debkumari, M. Favart, J. Fransaer, J. Vermant, and J. Michiels, Trends Microbiol. **16**, 496 (2008).

[28] D. López, H. Vlamakis, and R. Kolter, Cold Spring Harbor Perspect. Biol. **2**, a000398 (2010).

[29] D. Or, B. F. Smets, J. M. Wraith, A. Dechesne, and S. P. Friedman, Adv. Water Resour. **30**, 1505 (2007).

[30] A. Dechesne, G. Wang, G. Gülez, D. Or, and B. F. Smets, Proc. Natl. Acad. Sci. U.S.A. **107**, 14369 (2010).

[31] J. K. Struthers and R. P. Westran, *Clinical Bacteriology* (CRC Press, Boca Raton, 2003), p. 158.

[32] V. Ki and C. Rotstein, Can. J. Infect. Dis. Med. Microbiol. **19**, 173 (2008).

[33] R. R. Mercer, M. L. Russell, and J. D. Crapo, J. Appl. Phys. **77**, 1060 (1994).

[34] A. C. Rowat, D. E. Jaalouk, M. Zwerger, W. L. Ung, I. A. Eydelnant, D. E. Olins, A. L. Olins, H. Herrmann, D. A. Weitz, and J. Lammerding, J. Biol. Chem. **288**, 8610 (2013).

[35] S. Ramaswamy, Annu. Rev. Condens. Matter Phys. **1**, 323 (2010).

[36] T. Vicsek and A. Zafeiris, Phys. Rep. **517**, 71 (2012).

[37] P. Romanczuk, M. Bär, W. Ebeling, B. Lindner, and L. Schimansky-Geier, Eur. Phys. J. Spec. Top. **202**, 1 (2012).

[38] Y. Wu, Quant. Biol. **3**, 199 (2015).

[39] D. L. Koch and G. Subramanian, Annu. Rev. Fluid Mech. **43**, 637 (2011).

[40] K. Drescher, J. Dunkel, L. H. Cisneros, S. Ganguly, and R. E. Goldstein, Proc. Natl. Acad. Sci. U.S.A. **108**, 10940 (2011).

[41] S. D. Ryan, G. Ariel, and A. Be'er, Biophys. J. **111**, 247 (2016).

[42] See Supplemental Material at http://link.aps.org/supplemental/10.1103/PhysRevLett.119.018101 for supplemental methods and text that include Refs. [43–50], supplemental figures, and supplemental videos.

[43] N. Otsu, IEEE Trans. Systems Man Cybernetics **9**, 62 (1979).

[44] S. Maass *et al.*, Anal. Chem. **83**, 2677 (2011).

[45] L. S. Wong, M. S. Johnson, I. B. Zhulin, and B. L. Taylor, J. Bacteriol. **177**, 3985 (1995).

[46] H. C. Berg and D. A. Brown, Nature (London) **239**, 500 (1972).

[47] H. C. Berg and L. Turner, Biophys. J. **58**, 919 (1990).

[48] P. D. Frymier, R. M. Ford, H. C. Berg, and P. T. Cummings, Proc. Natl. Acad. Sci. U.S.A. **92**, 6195 (1995).

[49] A. P. Berke, L. Turner, H. C. Berg, and E. Lauga, Phys. Rev. Lett. **101**, 038102 (2008).

[50] G. Li and J. X. Tang, Phys. Rev. Lett. **103**, 078101 (2009).

[51] E. Lauga, W. R. DiLuzio, G. M. Whitesides, and H. A. Stone, Biophys. J. **90**, 400 (2006).

[52] S. E. Spagnolie and E. Lauga, J. Fluid Mech. **700**, 105 (2012).

[53] M. Molaei, M. Barry, R. Stocker, and J. Sheng, Phys. Rev. Lett. **113**, 068103 (2014).

[54] L. Turner, R. Zhang, N. C. Darnton, and H. C. Berg, J. Bacteriol. **192**, 3259 (2010).

[55] B. V. Jones, R. Young, E. Mahenthiralingam, and D. J. Stickler, Infect. Immun. **72**, 3941 (2004).

[56] M. F. Copeland, S. T. Flickinger, H. H. Tuson, and D. B. Weibel, Appl. Environ. Microbiol. **76**, 1241 (2010).

[57] K. M. Blair, L. Turner, J. T. Winkelman, H. C. Berg, and D. B. Kearns, Science **320**, 1636 (2008).

[58] R. A. Calvo and D. B. Kearns, J. Bacteriol. **197**, 81 (2015).

[59] S. Chattopadhyay, R. Moldovan, C. Yeung, and X. L. Wu, Proc. Natl. Acad. Sci. U.S.A. **103**, 13712 (2006).

[60] N. C. Darnton, L. Turner, S. Rojevsky, and H. C. Berg, J. Bacteriol. **189**, 1756 (2007).

[61] H. C. Berg, *Random Walks in Biology* (Princeton, Princeton, NJ, 1993).

[62] N. C. Darnton, L. Turner, S. Rojevsky, and H. C. Berg, Biophys. J. **98**, 2082 (2010).

[63] W. Kim, T. Killam, V. Sood, and M. G. Surette, J. Bacteriol. **185**, 3111 (2003).

[64] S. Lai, J. Tremblay, and E. Déziel, Environ. Microbiol. **11**, 126 (2009).

[65] M. T. Butler, Q. Wang, and R. M. Harshey, Proc. Natl. Acad. Sci. U.S.A. **107**, 3776 (2010).

[66] A. Finkelshtein, D. Roth, E. Ben Jacob, and C. J. Ingham, mBio **6**, e00074-15 (2015).

[67] S. M. Jacobsen, D. J. Stickler, H. L. Mobley, and M. E. Shirtliff, Clinical microbiology reviews **21**, 26 (2008).

[68] F. Peruani, A. Deutsch, and M. Bär, Phys. Rev. E **74**, 030904 (2006).

[69] A. Zöttl and H. Stark, Phys. Rev. Lett. **112**, 118101 (2014).

[70] N. Oyama, J. J. Molina, and R. Yamamoto, Phys. Rev. E **93**, 043114 (2016).

[71] H. Moore, K. Dvorakova, N. Jenkins, and W. Breed, Nature (London) **418**, 174 (2002).

[72] Y. Yang, J. Elgeti, and G. Gompper, Phys. Rev. E **78**, 061903 (2008).

[73] H. S. Fisher, L. Giomi, H. E. Hoekstra, and L. Mahadevan, Proc. R. Soc. B **281**, 20140296 (2014).